

Calculations of K^- nuclear quasi-bound states based on chiral meson-baryon amplitudes.

Daniel Gazda and Jiří Mareš

Nuclear Physics Institute, 250 68 Řež, Czech Republic

Abstract

In-medium $\bar{K}N$ scattering amplitudes developed within a new chirally motivated coupled-channel model due to Cieplý and Smejkal that fits the recent SIDDHARTA kaonic hydrogen $1s$ level shift and width are used to construct K^- nuclear potentials for calculations of K^- nuclear quasi-bound states. The strong energy and density dependence of scattering amplitudes at and near threshold leads to K^- potential depths $-\text{Re}V_K \approx 80 - 120$ MeV. Self-consistent calculations of all K^- nuclear quasi-bound states, including excited states, are reported. Model dependence, polarization effects, the role of p -wave interactions, and two-nucleon $K^- NN \rightarrow YN$ absorption modes are discussed. The K^- absorption widths Γ_K are comparable or even larger than the corresponding binding energies B_K for *all* K^- nuclear quasi-bound states, exceeding considerably the level spacing. This discourages search for K^- nuclear quasi-bound states in any but lightest nuclear systems.

Key words: K^- nuclear states, mesic nuclei, antikaon-nucleus interaction

PACS: 13.75.Jz, 21.65.Jk, 21.85.+d

1 Introduction

The study of the interaction of antikaons with baryonic systems, such as kaonic atoms, K^- nuclear clusters or dense strange kaonic matter, is an interesting issue with far-reaching consequences, e.g. for heavy-ion collisions and astrophysics. The closely related problem of K^- nuclear quasi-bound states is far from being settled, despite much theoretical and experimental effort in the last decade [1,2].

Our first studies of K^- quasi-bound states in nuclear many-body systems based on an extended relativistic mean field (RMF) model were focused on the widths expected for K^- quasi-bound states [3]. The subject of multi- K^- (hyper)nuclei was studied in Refs. [4,5,6] with the aim to explore whether kaon

condensation could occur in strong-interaction self-bound baryonic matter. In the RMF formulation, the energy independent real K^- nuclear potential was supplemented by a phenomenological imaginary potential fitted to kaonic atom data, with energy dependence that accounted for the reduced phase space available for in-medium K^- absorption, including 2-nucleon absorption modes.

Weise and Hartle performed calculations of K^- nuclear states in ^{16}O and ^{208}Pb using chiral-model $\bar{K}N$ amplitudes within a local density approximation [7].

This paper reports on our latest calculations of K^- nuclear quasi-bound states within a chirally motivated meson-baryon coupled-channel separable interaction model [8]. We apply a self-consistent scheme for constructing K^- nuclear potentials from subthreshold in-medium $\bar{K}N$ scattering amplitudes which was introduced in Refs. [9,10]. This time, the $\bar{K}N$ amplitudes are constructed using a recent in-medium coupled channel model NLO30 [11] that reproduces all available low energy $\bar{K}N$ observables, including the latest 1s level shift and width in the K^- hydrogen atom from the SIDDHARTA experiment [12]. We demonstrate the crucial role of the strong energy and density dependencies of the K^-N scattering amplitudes, leading to deep K^- nuclear potentials for various considered versions of in-medium modifications of the scattering amplitudes. Using several versions of the chirally motivated coupled-channel model, we demonstrate the model dependence of our calculations. Moreover, we discuss the effects of p -wave interactions and the $K^-NN \rightarrow YN$ absorption modes. Finally, we present binding energies and widths of *all* K^- quasi-bound states – including excited states – in selected nuclei.

The paper is organized as follows. In Section 2, we briefly describe the model and underlying self-consistent scheme for constructing K^- nucleus potentials from in-medium subthreshold $\bar{K}N$ scattering amplitudes. In Section 3, we present results of our calculations of K^- quasi-bound states in various nuclei across the periodic table. Conclusions are summarized in section 4.

2 Model

In this section, we briefly outline the methodology which forms the framework of our calculations of K^- nuclear quasi-bound states. We concentrate only on basic ingredients of the model since the details can be found in Refs. [9,10,11].

The K^- nuclear quasi-bound states are determined by self-consistent solution of the in-medium Klein–Gordon equation:

$$\left[\nabla^2 + \tilde{\omega}_K^2 - m_k^2 - \Pi_K(\omega_K, \vec{p}_K, \rho) \right] \phi = 0, \quad (1)$$

where $\tilde{\omega}_K$ is complex energy of antikaon containing the Coulomb interaction V_C introduced by minimal substitution:

$$\tilde{\omega}_K = \omega_K - i\Gamma_K/2 - V_C, \quad (2)$$

with Γ_K being the width of K^- nuclear state of energy $\omega_K = m_K - B_K$, where B_K is the binding energy of antikaon. The self-energy operator $\Pi_K = 2(\text{Re}\omega_K)V_K$ is constructed in a “ $t\rho$ ” form with the amplitude calculated in a chirally motivated coupled-channel approach:

$$\Pi_K(\omega_K, \vec{p}_K, \rho) = -4\pi \frac{\sqrt{s}}{m_N} \left[F_{K-p}(\sqrt{s}, \vec{p}, \rho) \rho_p + F_{K-n}(\sqrt{s}, \vec{p}, \rho) \rho_n \right], \quad (3)$$

where $F_{K-p(n)}$ is the K^- -proton (neutron) in-medium scattering amplitude in a separable form, \vec{p} is the relative K^-N momentum, and \sqrt{s} is the K^-N total energy. The realistic proton ρ_p and neutron ρ_n density distributions in the core nuclei are taken from relativistic mean-field nuclear-structure calculations. The K^-N scattering amplitudes F_{K-N} are constructed within a chirally motivated coupled-channel separable interaction model [8]. In this work, we applied the latest version NLO30 [11] which reproduces the recent K^- hydrogen $1s$ level shift and width from the SIDDHARTA experiment [12]. For the sake of comparison, we applied as well the TW1 model [10,11] fitted also to the SIDDHARTA data, and the older CS30 model [8]. It is to be noted that in the TW1 (NLO30, CS30) model, the effective separable meson-baryon potentials are constructed to match the equivalent amplitudes derived from the chiral effective Lagrangian at leading (next-to-leading) order, respectively.

When the elementary K^-N system is embedded in the nuclear medium of density ρ , one has to consider in-medium modifications of the scattering amplitude, in particular Pauli blocking in the intermediate states (this in-medium version is marked ‘no SE’) [13]. The other version (marked ‘+SE’) adds self-consistently meson and baryon self-energies generated by the interaction of hadrons with the nuclear medium [14,15].

Figure 1 illustrates a typical resonance-shape energy dependence of the in-medium reduced ¹ scattering amplitudes $f_{K-N}(\sqrt{s}, \rho) = 1/2[f_{K-p}(\sqrt{s}, \rho) + f_{K-n}(\sqrt{s}, \rho)]$ for nuclear matter density $\rho_0 = 0.17 \text{ fm}^{-3}$, corresponding to the interaction of the K^- meson with symmetric nuclear matter. The amplitudes were calculated within the TW1 and NLO30 models and for each of the models, two in-medium versions, ‘no SE’ and ‘+SE’, are shown for comparison. The pronounced energy dependence of the scattering amplitude appears crucial in the self-consistent calculations of kaonic nuclear states. In particular, the real part of the ‘+SE’ amplitudes in both models changes from weak

¹ $F_{K-N} = g(p)f_{K-N}g(p')$, see Ref. [10]

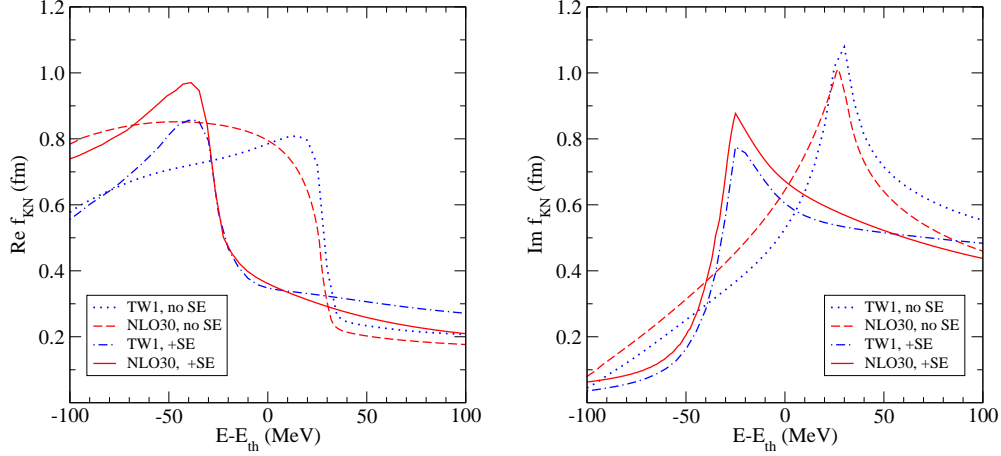


Fig. 1. Energy dependence of the c.m. reduced amplitude f_{K-N} in TW1 and NLO30 models (left: real part, right: imaginary part). Dotted and dashed lines: Pauli blocked amplitude (‘no SE’) for $\rho_0 = 0.17 \text{ fm}^{-3}$; solid and dot-dashed lines: including also hadron self-energies (‘+SE’) at ρ_0 .

attraction at and above threshold to strong attraction at $\sim 30 \text{ MeV}$ below threshold. As a result, the ‘+SE’ and ‘no SE’ amplitudes become close to each other at energies relevant for self-consistent calculations of kaonic nuclei. While both models give similar imaginary parts $\text{Im} f_{K-N}$ for each in-medium version, they differ considerably ($\approx 20\%$) in real parts of the scattering amplitudes below threshold. This indicates the extent of the model dependence of the calculations of K^- nuclear quasi-bound states.

The scattering amplitude F_{K-N} in Eq. (3) is a function of K^-N c.m. energy \sqrt{s} and relative momentum \vec{p} . For nuclear bound-state applications it is necessary to transform the two-body K^-N arguments into the \bar{K} -nuclear c.m. frame. For the relative momentum \vec{p} we have

$$\vec{p} = \xi_N \vec{p}_K - \xi_K \vec{p}_N, \quad \xi_{N(K)} = m_N(K)/(m_N + m_K), \quad (4)$$

which upon averaging over angles yields p^2 of the form

$$p^2 = \xi_N \xi_K \left(2m_K \frac{p_N^2}{2m_N} + 2m_N \frac{p_K^2}{2m_K} \right). \quad (5)$$

Similarly, expanding near threshold energy $E_{\text{th}} = m_K + m_p$, \sqrt{s} assumes the form

$$\sqrt{s} \approx E_{\text{th}} - B_K - V_C - B_N - \xi_N \frac{p_N^2}{2m_N} - \xi_K \frac{p_K^2}{2m_K}, \quad (6)$$

where B_N stands for the binding energy of nucleon, and the last two terms represent corrections due to the kinetic energies of nucleon and antikaon. The

nucleon kinetic energy is approximated in the Fermi gas model $p_N^2/(2m_N) = 23(\rho/\rho_0)^{2/3}$ MeV and the kinetic energy of antikaon is obtained by means of local density approximation $p_K^2/(2m_N) = -B_K - \text{Re } \mathcal{V}_K$, where $\mathcal{V}_K = V_K + V_C$. This finally leads to

$$p^2 \approx \xi_N \xi_K \left[2m_K 23 (\rho/\rho_0)^{2/3} - 2m_N (B_K + \text{Re } \mathcal{V}_K(\rho)) \right] \quad (\text{in MeV}), \quad (7)$$

$$\sqrt{s} \approx E_{\text{th}} - B_N - \xi_N B_K - 15.1 \left(\frac{\rho}{\rho_0} \right)^{2/3} + \xi_K \text{Re } \mathcal{V}_K(\rho) \quad (\text{in MeV}). \quad (8)$$

We note that the K^- potential V_K and the K^- binding energy B_K appear as arguments in the expression for \sqrt{s} , which in turn serves as an argument for the self-energy Π_K , and thus for V_K . This suggests a self-consistency scheme in terms of both V_K and B_K for solving the Klein-Gordon equation (1).

It is to be stressed that the present chiral model of K^- -nucleus interaction does not account for the absorption of K^- mesons in the nuclear medium through nonpionic conversion modes on two nucleons $K^- NN \rightarrow YN$ ($Y = \Lambda, \Sigma$). To estimate the contribution of two-nucleon absorption processes to the decay widths of K^- nuclear states we introduced phenomenological term into the K^- self-energy:

$$\text{Im } \Pi_K^{(2N)} = 0.2 f_{YN}(B_K) W_0 \rho^2, \quad (9)$$

where W_0 was fixed by kaonic atom data analysis and $f_{YN}(B_K)$ is kinematical suppression factor taking into account reduced phase space available for decay products of K^- nuclear bound states [3].

The present chiral model also does not address the p -wave part of the K^- -nucleus interaction. Since p -waves may play an important role for tightly bound K^- nuclear systems [16] we studied their contribution by adding the self-energy term:

$$\Pi_K^{(p)} = -4\pi \frac{m_N}{\sqrt{s}} \vec{\nabla} C_{K-N}(\sqrt{s}) \rho \cdot \vec{\nabla}, \quad (10)$$

with C_{K-N} p -wave amplitude constrained by the $\Sigma(1385)$ resonance phenomenology and parametrized following Ref. [7].

3 Results and discussion

We adopted the above methodology to calculations of quasi-bound K^- states in selected nuclei across the periodic table. In most cases, we solved KG equa-

tion self-consistently in a static approximation. For the sake of comparison, we performed also fully dynamical calculations upon taking into account the polarization of the nuclear core by the strongly bound antikaon.

Figure 2 shows the K^- nuclear potentials for $1s$ state in Ca at threshold (E_{th}) and for \sqrt{s} (Eq. (8)) calculated self-consistently with respect to $\text{Re}V_K$ and B_K , for TW1 amplitudes (upper panels) and NLO30 amplitudes (lower panels). The relevant values of B_K in Ca and other nuclei are presented in the following figures. It is seen that the subthreshold extrapolation \sqrt{s} is crucial for the depth of V_K , calculated using the TW1 amplitude in both ‘no SE’ and ‘+ SE’ in-medium version. While at threshold the depth of $\text{Re}V_K$ in the ‘+SE’ case is about half of the depth in the ‘no SE’ case, for \sqrt{s} both in-medium versions give a similar depth $-\text{Re}V_K(\rho_0) \approx 85 - 90$ MeV. In the case of the NLO30 model, the situation is rather different. While the self-consistent calculation is still important for the depth of $\text{Re}V_K$, evaluated using the ‘+SE’

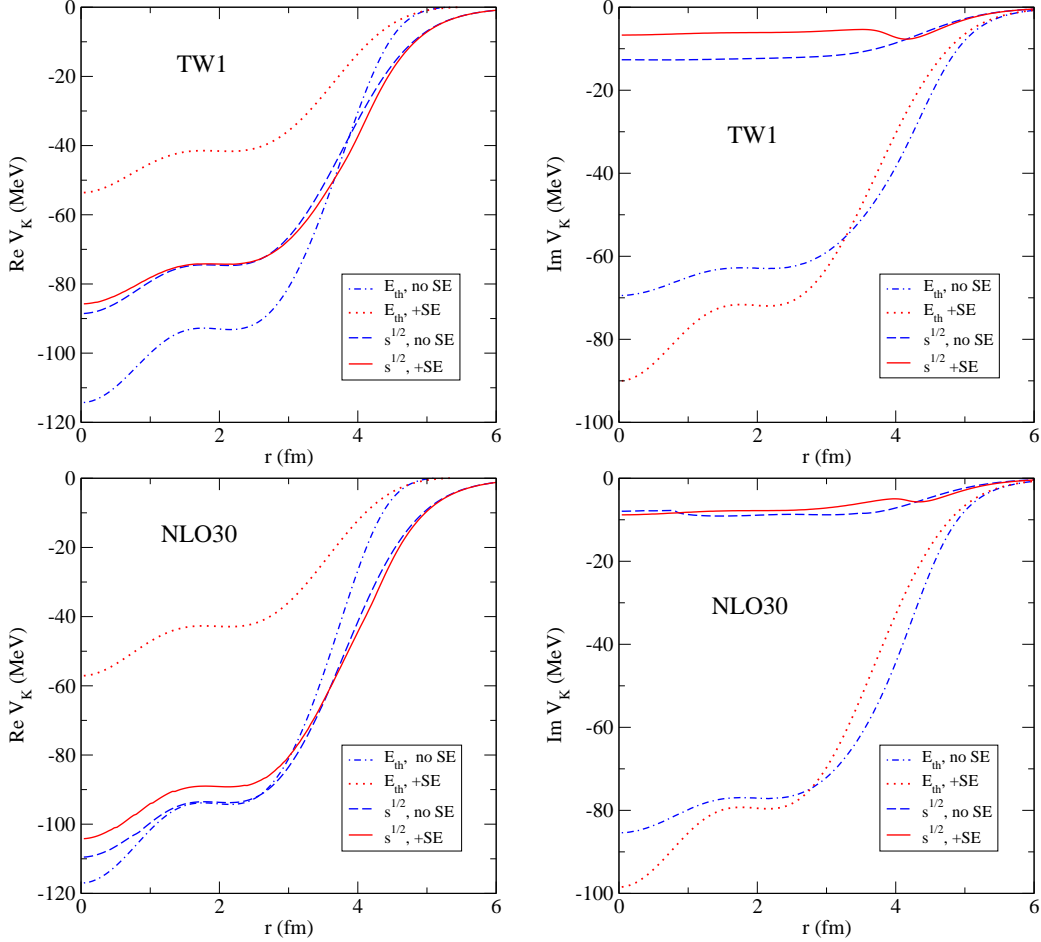


Fig. 2. K^- nuclear potentials in Ca (left: real part, right: imaginary part), calculated with static RMF nuclear densities and chiral amplitudes (upper panels: TW1, lower panels: NLO30) at threshold (E_{th}) and with \sqrt{s} , in both in-medium versions: only Pauli blocking (‘no SE’) and including also hadron self-energies (‘+SE’).

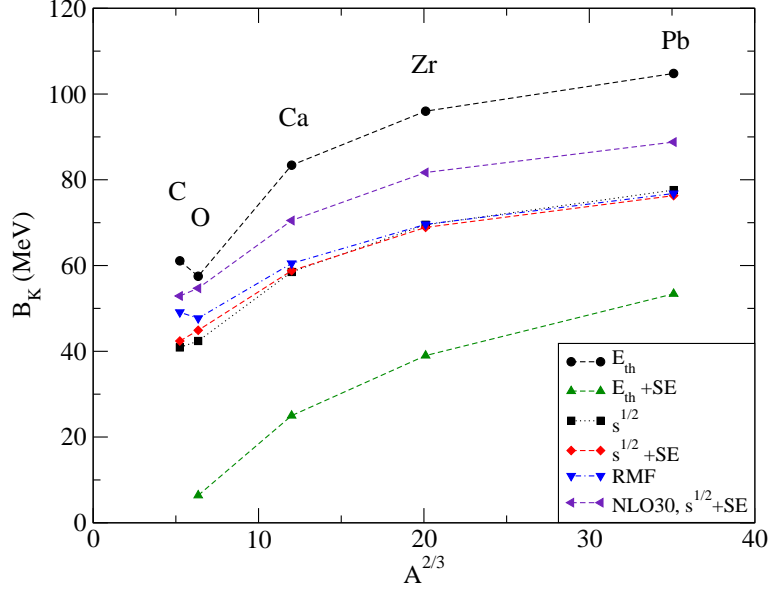


Fig. 3. Binding energies B_K of $1s$ K^- nuclear quasi-bound states in several nuclei, calculated using static RMF nuclear densities and TW1 chiral amplitudes at threshold (E_{th}) and with \sqrt{s} , in both in-medium versions: only Pauli blocking ('no SE') and including also hadron self-energies ('+SE'). Results of static RMF calculations, with a K^- nuclear interaction mediated by vector mesons only, as well as for NLO30 chiral '+ SE' amplitudes are shown for comparison.

in-medium modification, in the 'no SE' case, the depths of $\text{Re}V_K$ evaluated at threshold and at \sqrt{s} are close to each other. This weak energy dependence of $\text{Re}V_K$ has its origin in rather weak energy dependence of the 'no SE' NLO30 scattering amplitude below threshold, as shown in Fig. 1. The NLO30 model yields ~ 20 MeV deeper $\text{Re}V_K$ than the TW1 model, as could be anticipated from Fig. 1. The imaginary parts of V_K and consequently the widths which represent only $K^-N \rightarrow YN$ decays, are considerably reduced in the self-consistent calculations of the subthreshold amplitudes owing to the proximity of the $\pi\Sigma$ threshold (see both right panels of Fig. 2).

The peculiar role of the energy dependence of the K^-N scattering amplitudes is illustrated for the TW1 model in Fig. 3. Binding energies B_K of $1s$ K^- nuclear quasi-bound states obtained by solving Eq. (1) self-consistently (denoted ' $s^{1/2}$ ') for several nuclei are compared with B_K calculated using threshold amplitudes (E_{th}). It is worth noting that the self-consistent calculations of B_K using 'no SE' and '+SE' in-medium amplitudes give very similar results. These B_K values are remarkably close to those calculated within a static RMF approach, when the K^- -nucleus interaction is mediated exclusively by vector mesons with purely vector SU(3) F-type couplings (denoted 'RMF') [4]. For comparison, we present also binding energies B_K calculated self-consistently using the NLO30 '+SE' amplitudes which are more than 10 MeV larger than the corresponding binding energies calculated using the TW1 amplitudes.

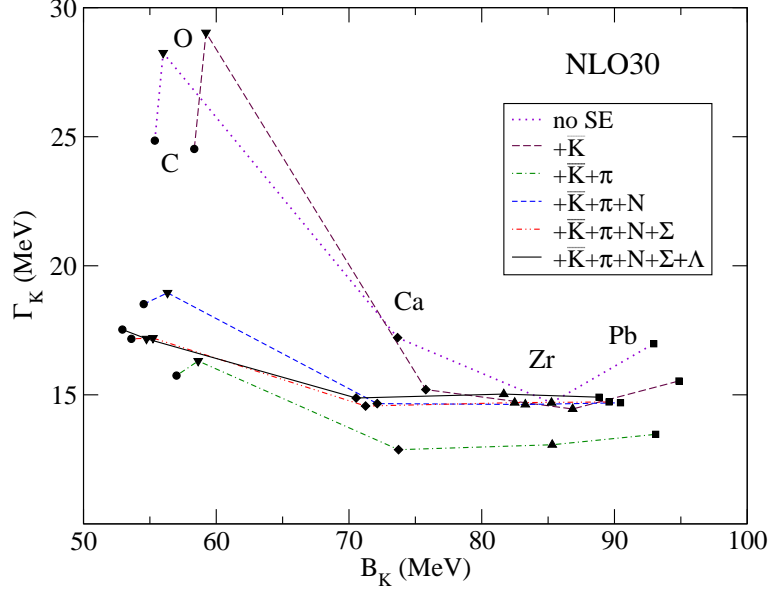


Fig. 4. Binding energies B_K and widths Γ_K of $1s$ K^- nuclear quasi-bound states, calculated self-consistently with static RMF nuclear densities and in-medium NLO30 amplitudes with various hadron self-energies considered in intermediate states (see the legend). $K^-NN \rightarrow YN$ decay modes are not included.

Figure 4 shows the effect of particular hadron self-energies in the intermediate states on the K^- binding energies B_K and widths Γ_K , calculated self-consistently within the NLO30 model. The widths Γ_K are plotted as function of B_K for various options of implementation of the self-energies, as indicated in the legend of Fig. 4. The binding energies B_K in all nuclei under consideration differ in all cases by less than 5 MeV and the effect of self-energies seems to be A independent. Implementation of pion self-energies leads to a sizable reduction of the widths Γ_K in lighter nuclei (C, O). On the other hand, the role of hyperon self-energies seems to be marginal.

It is to be noted that the calculated widths shown in the figure represent only $K^-N \rightarrow \pi Y$ decays, accounted for by the coupled-channel chiral model. When phenomenological energy dependent imaginary ρ^2 terms are added self-consistently to simulate two-nucleon $K^-NN \rightarrow YN$ absorption modes and their available phase space [3], the resulting widths of order $\Gamma_K \approx 50$ MeV become comparable in light nuclei to the binding energies B_K .

Figure 5 illustrates the model dependence of the K^- nuclear state calculations by presenting B_K and Γ_K of $1s$ K^- states in selected nuclei calculated self-consistently using various chiral-model scattering amplitudes – TW1, CS30, and NLO30. The CS30 and NLO30 models yield larger binding energies and lower widths of the nuclear K^- quasi-bound states than the TW1 model. The differences between the chiral models are up to 20 MeV in the binding energies and up to 10 MeV in the widths. The model dependence of B_K and Γ_K

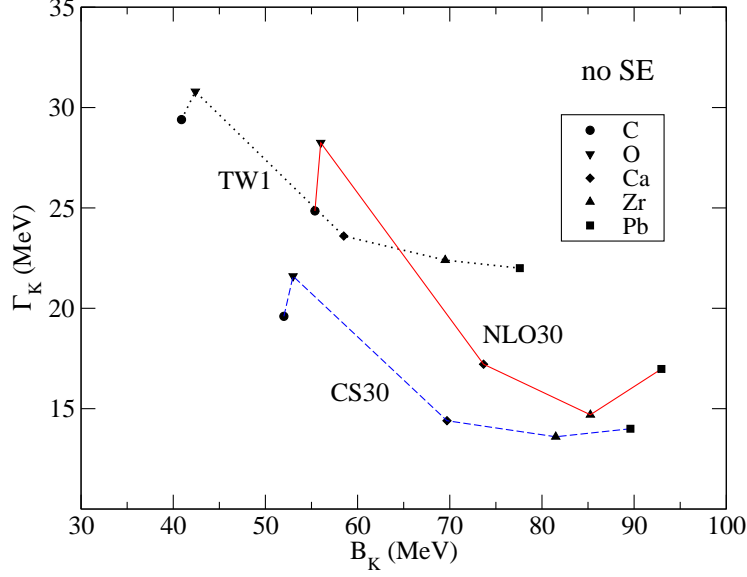


Fig. 5. Binding energies B_K and widths Γ_K of $1s$ K^- nuclear quasi-bound states, calculated self-consistently with static RMF densities and the ‘no SE’ TW1, CS30 and NLO30 scattering amplitudes. $K^-NN \rightarrow YN$ decay modes are not included.

is thus more pronounced than the effects of self-energies in the self-consistent calculations of kaonic nuclei.

Figure 6 shows binding energies and widths of K^- quasi-bound states – including excited states – in selected nuclei calculated by applying self-consistently the subthreshold extrapolations \sqrt{s} of Eq. (8) to the NLO30 ‘+SE’ amplitudes. Clearly, the widths of higher excited states are appreciable, exceeding the corresponding level spacing, even in the case when $2N$ absorption is not

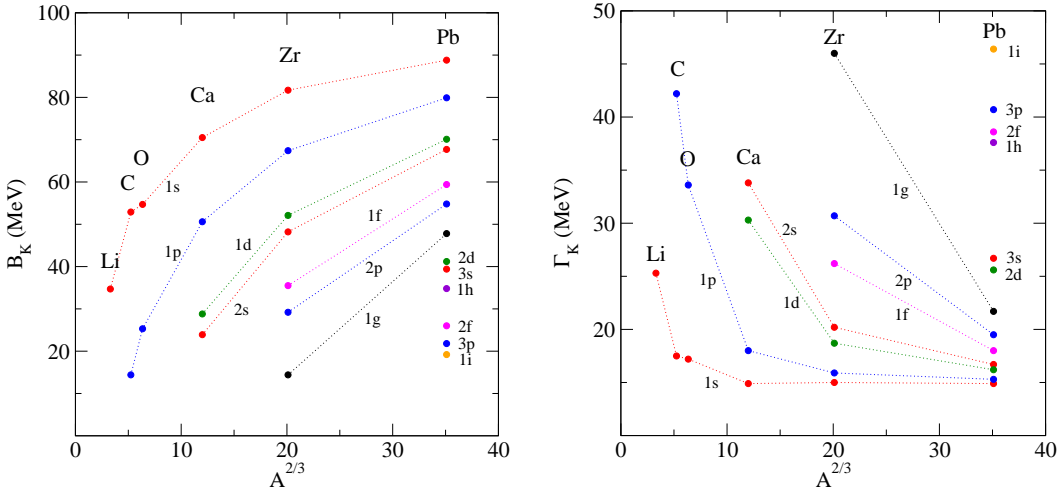


Fig. 6. Binding energies B_K (left panel) and widths Γ_K (right panel) of K^- quasi-bound states in selected nuclei, calculated self-consistently with static RMF densities and the ‘+ SE’ NLO30 scattering amplitudes. $K^-NN \rightarrow YN$ decay modes are not included.

considered. This leads to considerable overlap of the K^- quasi-bound states even in the lightest nuclei (except Li, where only the $1s$ K^- quasi-bound state exists). It is to be stressed that the $2N$ absorption which was not considered here, adds additional sizable contribution to the widths, particularly of low lying states. Such large widths thus inevitably obscure experimental study of the K^- nuclear quasi-bound states in heavier nuclei.

Table 1 shows, as representative examples, binding energies B_K and widths Γ_K of K^- nuclear quasi-bound states in Ca, calculated self-consistently using the NLO30 ‘+SE’ scattering amplitudes. The results of fully dynamical RMF calculations which take into account the polarization of the nuclear core by the strongly bound K^- meson, are compared with the static RMF scheme in the first 2 blocks. The dynamical calculations give, in general, higher binding energies B_K and smaller widths Γ_K . As could be anticipated, the polarization effect is A dependent: while it increases B_K by ~ 6 MeV in Li, it is less than 2 MeV in Ca (shown in Table 1), and in Pb the difference between static and dynamical calculations is less than 0.5 MeV. Effects of adding a p -wave K^-N interaction assigned to the $\Sigma(1385)$ resonance are demonstrated within the static RMF scheme in the third block of the table. The p -wave interaction increases the K^- binding energy only by few MeV, being more pronounced in light nuclei where surface effects are relatively more important. Nevertheless, even in Pb the p -wave interaction increases B_K by ~ 2 MeV. Finally, phenomenological energy dependent imaginary ρ^2 terms are included to simulate $2N$ absorption processes $K^-NN \rightarrow YN$. Whereas the K^- binding energies B_K decrease only slightly, the absorption widths $\Gamma_K > 50$ MeV become comparable to the binding energies B_K or even much larger in the case of higher K^- nuclear quasi-bound states.

Table 1

Binding energies B_K and widths Γ_K (in MeV) of the K^- nuclear quasi-bound states in Ca, calculated self-consistently using NLO30 ‘+SE’ amplitudes. Dynamical and static RMF schemes are compared in the first two blocks. Results of a static RMF scheme including p -wave amplitudes is shown in the third block, and $K^-NN \rightarrow YN$ decay modes are included in the last block (‘+2N abs.’).

	dynamical		static		stat. + p wave		stat. + $2N$ abs.	
	B_K	Γ_K	B_K	Γ_K	B_K	Γ_K	B_K	Γ_K
$1s$	72.3	14.8	70.5	14.9	73.0	14.8	68.9	58.9
$1p$	52.8	17.7	50.6	18.0	53.1	17.9	49.2	53.6
$1d$	30.5	29.2	28.8	30.3	32.1	29.3	27.7	59.7
$2s$	24.6	30.9	23.9	33.8	26.3	34.2	21.6	67.1

4 Conclusions

We performed extensive study of the K^- nuclear quasi-bound states within a chirally motivated meson-baryon coupled-channel separable interaction model. We considered two in-medium versions of the K^-N scattering amplitudes: the ‘no SE’ version which takes into account only Pauli blocking in the intermediate states, and the ‘+SE’ version which adds self-consistently hadron self-energies. In addition, we used several versions of the model to explore model dependence of our calculations. In this contribution, we demonstrate on few selected examples main results of the calculations with the aim to assess the role of various ingredients of the approach that influence binding energies and widths of the K^- nuclear states. Energy dependence of the in-medium scattering amplitudes, particularly in the K^-N subthreshold region, is the decisive mechanism that controls the self-consistent evaluation of corresponding K^- optical potentials. While the two in-medium versions of the K^-N scattering amplitudes yield considerably different potential depths $\text{Re}V_K$ at threshold, they give similar depths in the self-consistent calculations with the subthreshold extrapolation of \sqrt{s} . The role of hadron self-energies in the self-consistent calculations of the K^- binding energies B_K is less pronounced than the model dependence of predicted B_K which amounts to $\Delta B_K \approx 15$ MeV. As for the calculated widths Γ_K , the model dependence and the effects due to the hadron self energies are comparable. The p-wave interaction generated by the $\Sigma(1385)$ subthreshold resonance was found to play only a marginal role.

The widths of low-lying K^- states due to $K^-N \rightarrow \pi Y$ conversions are substantially reduced in the self-consistent calculations, thus reflecting the proximity of the $\pi\Sigma$ threshold. On the contrary, the widths of higher excited K^- states are quite large even if only the pion conversion modes on a single nucleon are considered. After including 2 body $K^-NN \rightarrow YN$ absorption modes, the total decay widths Γ_K are comparable or even larger than the corresponding binding energies B_K for *all* K^- nuclear quasi-bound states, exceeding considerably the level spacing.

The above conclusions should discourage attempts to search for isolated peaks corresponding to K^- nuclear quasi-bound states in any but very light nuclear systems.

Acknowledgements

We wish to acknowledge a fruitful collaboration with Aleš Cieplý, Eli Friedman and Avraham Gal. This work was supported by the GACR grant No. 202/09/1441 and by the EU initiative FP7, HadronPhysics2, under project No. 227431.

References

- [1] See contributions in: A. Gal, R. S. Hayano (Eds.), *Recent Advances in Strangeness Nuclear Physics*, Nucl. Phys. A 804 (2008) 171-348.
- [2] See contributions in: B. F. Gibson, K. Imai, T. Motoba, T. Nagae, A. Ohnishi (Eds.), *Proc. 10th Int. Conf. on Hypernuclear and Strange Particle Physics*, Tokai, 14-18 September 2009, Nucl. Phys. A 835 (2010) 1-469.
- [3] J. Mareš, E. Friedman, A. Gal, Nucl. Phys. A 770 (2006) 84.
- [4] D. Gazda, E. Friedman, A. Gal, J. Mareš, Phys. Rev. C 76 (2007) 055204.
- [5] D. Gazda, E. Friedman, A. Gal, J. Mareš, Phys. Rev. C 77 (2008) 045206.
- [6] D. Gazda, E. Friedman, A. Gal, J. Mareš, Phys. Rev. C 80 (2009) 035205.
- [7] W. Weise, R. Härtle, Nucl. Phys. A 804 (2008) 173.
- [8] A. Cieplý, J. Smejkal, Eur. Phys. J. A 43 (2010) 191.
- [9] A. Cieplý, E. Friedman, A. Gal, D. Gazda, J. Mareš, Phys. Lett. B 702 (2011) 402.
- [10] A. Cieplý, E. Friedman, A. Gal, D. Gazda, J. Mareš, Phys. Rev. C 84 (2011) 045206.
- [11] A. Cieplý, J. Smejkal, Nucl. Phys. A 881 (2012) 115.
- [12] M. Bazzi *et al.* (SIDDHARTA Collaboration), Phys. Lett. B 704 (2011) 113;
M. Bazzi *et al.* (SIDDHARTA Collaboration), Nucl. Phys. A 881 (2012) 88.
- [13] T. Waas, N. Kaiser, W. Weise, Phys. Lett. B 365 (1996) 12;
T. Waas, N. Kaiser, W. Weise, Phys. Lett. B 379 (1996) 34.
- [14] M. Lutz, Phys. Lett. B 426 (1998) 12.
- [15] A. Ramos, E. Oset, Nucl. Phys. A 671 (2000) 481.
- [16] S. Wycech, A. M. Green, Phys. Rev. C 79 (2009) 014001.